Solid-State Electronics Vol. 24, pp. 455–459, 1981
Printed in Great Britain. All rights reserved

0038-1101/81/050455-05$02.00/0
Copyright © 1981 Pergamon Press Ltd.

NUMERICAL ANALYSIS ON ABNORMAL THYRISTOR FORWARD VOLTAGE INCREASE DUE TO HEAVY DOPING IN GATED *P*-BASE LAYER

AKIO NAKAGAWA
Toshiba Research and Development Center, 1, Komukai Toshibacho, Saiwaiku, Kawasaki 210, Japan

(*Received* 4 *February* 1980; *in revised form* 31 *May* 1980)

Abstract—An abnormal forward voltage increase was observed for a p-base gated double diffused $n^+pn^-p^+$ high power thyristor with high impurity concentration at the n^+–p emitter-base junction. Accurate numerical analysis shows that heavy doping effects are the most responsible mechanism for the abnormality and that depletion layer formation at the center junction accompanies it.

It will be shown that appropriate control of the impurity concentration at the emitter-base junction is necessary to avoid this abnormality by realizing the common base transistor current gain of greater than 0.73 for n^+pn^--portion.

NOTATION

- q unit charge
- k Boltzmann's constant
- T temperature
- N_D, N_A donor and acceptor densities
- n_i, ω parameters characterizing heavy doping effects
- n_{ro}^2 electron-hole product in thermal equilibrium
- n, p electron and hole densities
- J_n, J_p electron and hole current densities
- ψ electrostatic potential
- μ_n, μ_p electron and hole mobilities
- τ_n, τ_p carrier lifetimes for electron and hole
- R, G recombination and generation rate
- C_{EB} impurity concentration at n^+–p emitter-base junction
- $\alpha_{npn}, \alpha_{pnp}$ common base transistor current amplification factors for n^+pn^- three layers and p^+n^-p three layers for the four thyristor layers $n^+pn^-p^+$

1. INTRODUCTION

Recently, heavy doping effects (band gap narrowing) have been studied by many authors[1–7]. It was found that, introducing heavy doping effects successfully explains low injection efficiency for a bipolar transistor with heavily doped emitter and base[1, 2]. For thyristors, Adler has recently shown heavy doping effects on current-voltage characteristics, using an accurate numerical model[8].

The present paper reports results obtained from studying heavy doping effects numerically on a p-base-gated double-diffused high power thyristor. Usually, a double-diffused thyristor has an $n^+pn^-p^+$ four layer structure. The first three layers, n^+pn^-, have a similar impurity profile to that of a double-diffused transistor. It was shown[3, 9] that high impurity concentration C_{EB} at the emitter-base junction of a diffused transistor significantly reduces its emitter injection efficiency. Thyristor current-voltage characteristics are thus necessarily sensitive to impurity concentration C_{EB} at the n^+–p emitter-base junction.

Figure 1 shows a typical current-voltage characteristic for a thyristor with a high impurity concentration C_{EB} of 2.1×10^{18}. An abrupt forward voltage increase is seen at

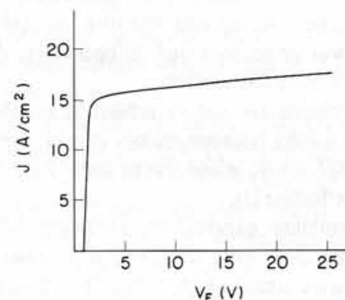

Fig. 1. Measured current–voltage characteristic for a thyristor with a high C_{EB} value.

the low current density around 15 A/cm^2. This is a far different current-voltage characteristic from that of an ordinary thyristor, but quite similar to a transistor current-voltage characteristic. Nevertheless, this is still a kind of thyristor current-voltage characteristics, because no gate current is necessary to sustain its conduction state. The detailed abnormal characteristics were experimentally obtained by Azuma *et al.* as a joint research and the result will be separately published[10].

In order to analyze the abnormality in the following chapters, numerical analysis will be carried out using a heavy doping model developed in Refs. [3, 4].

2. ONE DIMENSIONAL MATHEMATICAL MODEL

Thyristor numerical simulation was given first by Anheier *et al.*[11], and independently by Kurata[12]. An accurate numerical model was recently given by Adler[8], as already mentioned, including heavy doping effects, heat flow and various effects.

The present model also includes miscellaneous higher order effects: heavy doping effects, degeneracy effects, impurity concentration dependent carrier lifetime, carrier to impurity scattering, carrier to carrier scattering, and Auger recombination[3, 4, 8].

Transport equations, based on the heavy doping model under Fermi statistics, are given as follows[3], and

depend on the assumptions of quasi-equilibrium, complete ionization and isothermal condition.

$$J_P = -kT\mu_p \frac{\partial p}{\partial x} - q\mu_p p \frac{\partial \psi_1}{\partial x}, \quad (1)$$

$$J_n = kT\mu_n \frac{\partial n}{\partial x} - q\mu_n n \frac{\partial \psi_2}{\partial x}, \quad (2)$$

$$\psi_1 = \psi + \omega - \frac{kT}{q} \ln n_i/n_o, \quad (3)$$

$$\psi_2 = \psi + \omega + \frac{kT}{q} \ln n_i/n_o, \quad (4)$$

$$\frac{1}{q}\frac{\partial J_p}{\partial x} = -\frac{1}{q}\frac{\partial J_n}{\partial x} = G - R, \quad (5)$$

where n_i and ω are the characteristic quantities representing the magnitude of heavy doping effects and the discrepancy between Fermi statistics and Boltzmann statistics and n_0 is a given constant having the same dimension as n_i. The characteristic parameters depend on the local carrier density and impurity concentration, so that these will be recalculated, if necessary, during the course of iterative calculation.

Fermi statistics are not so influential on the present calculation results because excess carrier densities are below 1×10^{19}, above which Fermi statistics were shown to become effective[3].

Carrier mobility expressions, including field dependence, carrier to impurity scattering and carrier to carrier scattering, were obtained from [8]. The adopted recombination form is shown in eqn (6).

$$R = C(n^2p + p^2n) + \frac{np - n_{io}^2}{\tau_p(n + n_{io}) + \tau_n(p + n_{io})} \quad (6)$$

$$1/\tau_p = 1/\tau_n = 1/\tau_i + 1/\tau \quad (7)$$

$$\tau_i = 3 \times 10^{-6} \frac{1 \times 10^{18}}{N_D + N_A} (\text{sec}) \quad (8)$$

Auger coefficient C is taken as 2×10^{-31} cm^2/sec[8]. Impurity dependent carrier lifetime expressions (7 and 8) were obtained from [3 and 11]. n^- base carrier lifetime value τ is measured as 10 μsec by diode voltage decay method.

For boundary conditions, electrostatic potential values at both surface electrodes were given, and infinite recombination rate at both surfaces was assumed. Numerical calculations were carried out by usual Newton–Raphson iteration scheme[13, 14]. Thyristor current density is generally a multifunction of the applied voltage, so that a special calculation procedure is necessary to obtain the current–voltage characteristics. Initially, a low impurity concentration layer n^- is treated as an opposite impurity layer p^- so that the problem is reduced to $n^+pp^-p^+$ diode calculation. When carrier densities become greater than the impurity concentration in the n^- layer, the profile is switched to the real one. The next problem is to obtain the holding current. First the applied voltage was lowered until convergence is lost, then the applied voltage was reraised while giving appropriate ψ trial values.

3. CALCULATION RESULTS AND A COMPARISON WITH EXPERIMENTS

Table 1 shows the impurity diffusion parameters for 4 high power thyristors A, B, C and D. The impurity distributions will be assumed to be Gaussian in the present calculation. As devices with high C_{EB} values have low common base transistor current amplification factor α_{npn} for the first three layers n^+pn^-, a high τ value of 10 μsec in n-base layer was realized to obtain a latch-on $\alpha_{npn} + \alpha_{pnp} \geq 1.0$ condition, where α_{pnp} denotes the current amplification factor for the other three layers p^+n^-p.

Figure 2 shows a series of calculation results for thyristor C. Curve 1 is the result calculated by the present model. Curves 2–4 are results (2) without heavy doping effects, (3) without heavy doping effects and Auger recombination and (4) without heavy doping effects, Auger recombination and carrier to carrier scattering, respectively. Theoretical Curve 1 is in fairly good agreement with measured 0.4 A/cm^2 holding current and 15 A/cm^2 current density at 3 V. The calculation results

Table 1.

Samples	n-emitter diffusion		p-emitter and p-base diffusion		n^- base		C_{EB}
	surface conc. (cm^{-3})	depth (μm)	surface conc. (cm^{-3})	depth (μm)	impurity conc. (cm^{-3})	width (μm)	
A	2.5x10^{20}	15.4	2.66x10^{18}	55.2	2x10^{14}	150	1.27x10^{18}
B	4.0x10^{20}	11.6	2.75x10^{18}	53.5	2x10^{14}	150	1.79x10^{18}
C	5 x 10^{20}	9.2	2.8 x10^{18}	52.5	2x10^{14}	150	2.09x10^{18}
D	5 x 10^{20}	9.2	*2.8 x10^{17} (2.8 x10^{18})	52.5	2x10^{14}	150	2.24x10^{17}

*Device D is an imaginary one, and has different surface concentration: 2.8 x 10^{17} for base diffusion and 2.8 x 10^{18} for p-emitter diffusion.

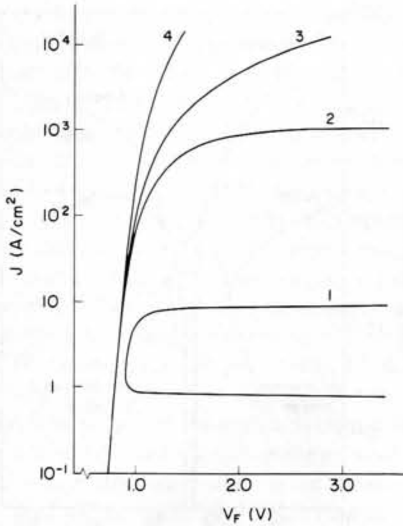

Fig. 2. Thyristor current–voltage characteristics under various hypothetical conditions. (1) Present model, (2) without heavy doping effects (H.D.E.), (3) without H.D.E. and Auger recombination and (4) without H.D.E. Auger recombination and carrier–carrier scattering.

without heavy doping effects exhibit a too low holding-current density, 1.5×10^{-3} A/cm², and too high current density at 3 V. Heavy doping effects are considered to be most responsible for the abnormal forward voltage increase for the present case.

Figure 3 shows calculated current voltage characteristics about thyristors A, B and C, which have C_{EB} values of 1.3×10^{18}, 1.8×10^{18} and 2.1×10^{18}, respectively. It is clearly seen that, as the C_{EB} value increases, the normal operation current density region is reduced. If the C_{EB} value further increases, the normal conduction area will vanish and such devices cannot latch on.

Figure 4 shows experimental and calculated current densities at a forward voltage of 3 V, where an abrupt forward voltage increase has already occurred, vs C_{EB} value. Though calculated values are slightly lower than

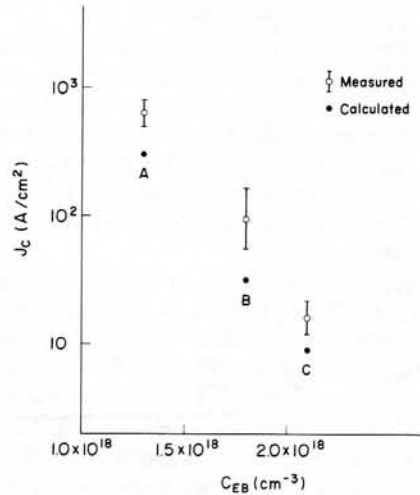

Fig. 4. Calculated and experimental current density J_c at 3 V forward voltage vs C_{EB} value.

the experimental ones, a fairly good agreement is obtained. In order to obtain sufficiently low forward voltage at high current density region, C_{EB} value is required to be small.

Figure 5 demonstrates carrier distributions inside device C for a series of applied voltages. Figure 6 shows electric field in the two bases for the same device. As the applied voltage increases, minimum carrier densities in the p-base decrease because of the high electric field appearing around the center junction. Detailed charge distributions around the center junction are given in Fig. 7, for 1.05 V. It is seen that net space charges, thus consequently the electric field, are formed mostly by ionized acceptors and mobile holes. In the region where net electric charge is negative, the acceptor density is more than 10 times as high as the mobile electron density. Corresponding results for 2.0 V are given in Fig. 8, showing that in the center junction vicinity, electron or hole density is less than that of acceptor or donor, respectively. Namely, a complete depletion layer is ap-

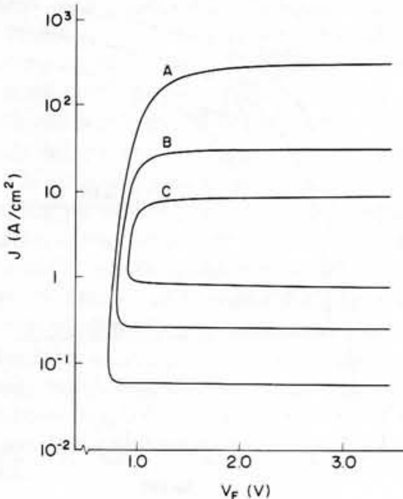

Fig. 3. Calculated current–voltage characteristics for thyristors A, B and C listed in Table 1.

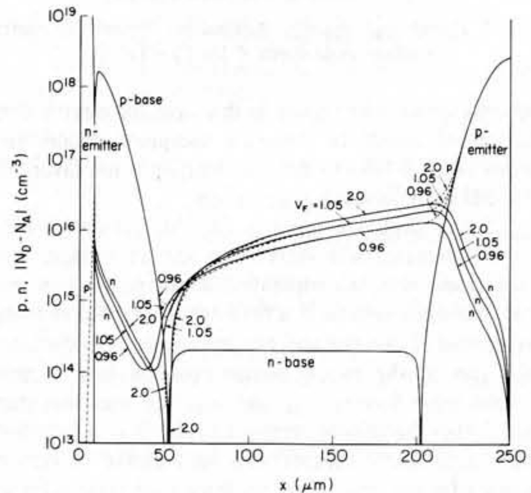

Fig. 5. Carrier densities p and n distributions inside device C with applied voltage as a parameter.

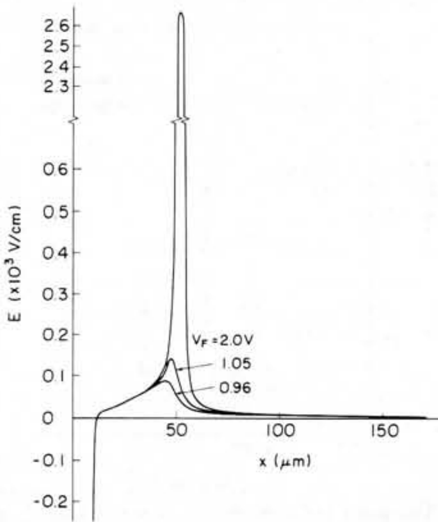

Fig. 6. Electric field inside device C with applied voltage as a parameter.

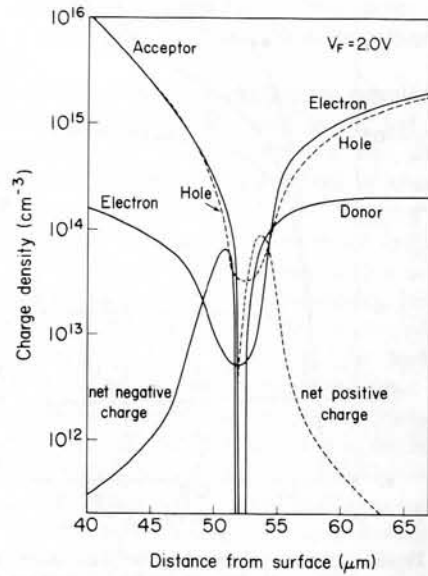

Fig. 8. Carrier and impurity distributions around the center junction inside device C for $V_F = 2.0$ V.

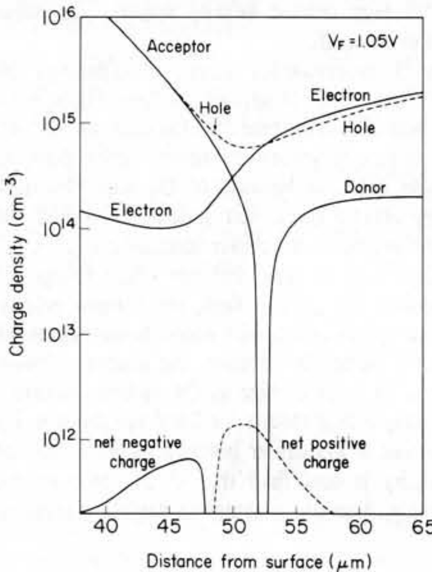

Fig. 7. Carrier and impurity distributions around the center junction inside device C for $V_F = 1.05$ V.

pearing in the same region. In this case, the electric field is formed mostly by immobile acceptors, donors and holes in the n-base so that the situation is not favorable for efficiently increasing the current.

After a depletion layer is formed, current density hardly increases with increase in applied voltage. This fact means complete separation of thyristor-action into two transistor-actions. If a thyristor is regarded as being composed of two *npn* and *pnp* transistors, it follows that the sum of the two transistor common base current amplification factors α_{npn} and α_{pnp} becomes less than unity over the critical current density. It is α_{pnp} rather than α_{npn} that decreases with an increase in current density for this case. There are three main reasons for its reduction: mobility reduction due to carrier to carrier scattering, increase in recombination rate due to Auger recombination and decrease in injection efficiency on account of n-base conductivity modulation.

The current density where the abnormality appears depends significantly on C_{EB} value, as already shown in Fig. 4. For devices with a low C_{EB} value, the depletion layer formation cannot be seen for any current density levels. Figure 7 shows this example. It shows the current-voltage characteristics for a series of carrier lifetime τ for device D with low C_{EB} value of 2.24×10^{17}. As the carrier lifetime decreases, the holding current density increases significantly. No abrupt forward voltage increase is seen for any carrier lifetime cases. These current-voltage characteristic variations are ordinary ones and frequently experienced.

In the following, discussions are given as to where the minimum carrier densities appear in the device (except for two emitters). A high electric field will appear around

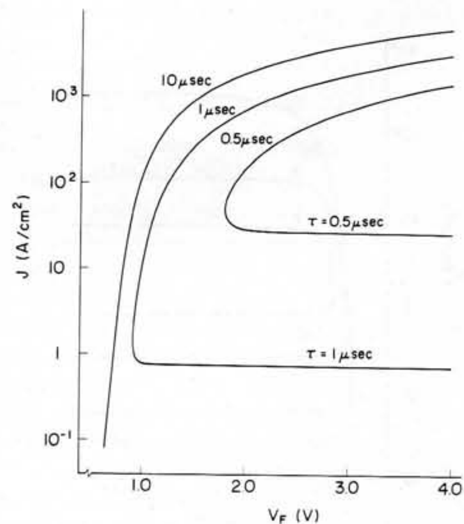

Fig. 9. Calculated current–voltage characteristics for thyristor D with carrier lifetime τ as a parameter.

the carrier density minimum points. Assume a high injection case, wherein both carrier densities in the n-base are greater than the n-base inpurity concentration and almost equal to each other and their distributions are determined by an ambipolar diffusion length[15]. In addition, the location of the lowest carrier densities is assumed to be in the n-base. In this location, electron and hole currents flow only by drift, because $\partial n/\partial x$ and $\partial p/\partial x$ are equal to zero. Thus, the current ratio J_n/J_p is equal to mobility ratio μ_n/μ_p there, whose value is usually around 2.7. Then, the ratio J_n/J_p at the center junction must be greater than 2.7, in this case. Conversely, if J_n/J_p at the center junction is greater than 2.7, the lowest hole density can be shown to be in the n-base. On the contrary, if ratio J_n/J_p at the center junction is less than 2.7, the lowest hole and electron densities must exist in different places from each other in the p-base. A high electric field will be applied between minimum hole and electron density locations. Roughly speaking, the J_n/J_p ratio at the center junction can be approximated as $\alpha_{npn}/\alpha_{pnp}$. It can, thus, be concluded that for a device with $\alpha_{npn}/\alpha_{pnp} < 2.7$, the lowest carrier densities appear in the p-base.

Accordingly, for devices with high C_{EB} value, thus low α_{npn}, the minimum electron density appears in the p-base and minimum hole density appears near the center junction in the p-base. The sum of alphas for a power thyristor is near unity because the value of α_{pnp} is relatively low due to its long n-base. Consequently, if the current amplification factor decreases, a high electric field will appear around the carrier density minimum points. The field will be formed mostly by immobile ionized acceptors and mobile holes, because electron current in the p-base flows by diffusion and the density is much less than the acceptor density. Thus, the high electric field will decrease minimum carrier densities and finally form a depletion layer.

On the contrary, for the devices with low C_{EB} value and thus, high α_{npn}, the location of the lowest carrier densities must be in the n-base, where almost all charges are mobile ones, so that carrier density distribution depends on the ambipolar diffusion length. Thus, even if carrier lifetime in the n-base is low, only high voltage drop occurs in the n-base. A depletion layer cannot appear at the center junction unless current ratio J_n/J_p at the center junction decreases below 2.7 with an increase in current density, because ratio J_n/J_p in the n-base is required to be smaller than 2.7 for holes in the n-base to form the highest electric field at the center junction. For most cases, carrier density in the p-base can exceed p-base impurity density in high current density levels. In this case, the device can be regarded as a p–i–n diode, and no separation into two transistors ever occurs.

The condition $\alpha_{npn}/\alpha_{pnp} > 2.7$ can be reduced to $\alpha_{npn} > 0.73$, using the latch-on condition $\alpha_{npn} + \alpha_{pnp} \geq 1$. Thus, the condition $\alpha_{npn} > 0.73$ is preferable as a thyristor design rule from a high surge current handling capability viewpoint.

4. CONCLUSION

The obtained characteristics for power thyristors with high C_{EB} value are quite strange, and are similar to the current-voltage characteristics for usual transistors, except for existence of a holding current. The most different point is that they do not need any gate current to sustain their conduction state, because one of the collector currents is the base current of the other transistor.

The current density where the abrupt forward voltage increase occurs depends strongly on both the C_{EB} value and the carrier lifetime τ. Thus, appropriate control of the C_{EB} value will be necessary for thyristor high-surge-current handling capability, in order to realize high α_{npn} and avoid the abnormality.

Calculations carried out in the present paper could successfully reproduce the abrupt forward voltage increase due to high C_{EB} value, in spite of many assumptions introduced concerning heavy doping model, carrier-to-carrier scattering and impurity-dependent carrier lifetime etc.

The author considers that the discrepancy in the present calculations and experiments should mainly be attributed to the heavy doping model and mobility expressions, because it was shown in Fig. 11 in Ref. [3] that the present heavy doping model gives slightly lower transistor current gain when compared with experiments, and because the mobility expressions used are very tentative for carrier-to-carrier scattering and for the degeneracy case.

Acknowledgements—The author thanks Dr. M. Kurata for useful discussions with him and his support for this work, and Mr. M. Azuma for providing data for Fig. 4.

REFERENCES

1. H. J. DeMan, *IEEE Trans. Electron. Dev.* **ED-18**, 833 (1971).
2. R. Van Overstraeten, H. J. De Man and R. Mertens, *IEEE Trans Electron. Dev.* **ED-20**, 290 (1973).
3. A. Nakagawa, *Solid-St. Electron.* **22**, 943 (1979).
4. M. S. Mock, *Solid-St. Electron.* **16**, 1251 (1973).
5. M. S. Mock, *Solid-St. Electron.* **17**, 819 (1974).
6. R. Mertens, H. J. De Man and R. Van Overstraeten, *IEEE Trans Electron. Dev.* **ED-20**, 772 (1973).
7. J. W. Slotboom and H. C. De Graaff, *Solid-St. Electron.* **19**, 857 (1976).
8. M. S. Adler, *IEEE Trans Electron. Dev.* **ED-25**, 16 (1978).
9. M. Azuma, A. Nakagawa and K. Takigami, *Jap. J. Appl. Physics* **17**(1), 257 (1977).
10. M. Azuma and K. Takigami, IEEE Electron Device Letters EDL-1, 203 (1980).
11. W. Anheier, W. L. Engl, O. Manck and A. Wieder, *IEDM Technical Digest*, pp. 363–366, Washington DC (1–3 Dec. 1975).
12. M. Kurata, *Solid-St. Electron.* **19**, 527 (1976).
13. D. L. Scharfetter and H. K. Gummel, *IEEE Trans Electron. Dev.* **ED-16**, 64 (1969).
14. M. Kurata, *IEEE Trans Electron. Dev.* **ED-19**, 1207 (1972).
15. H. R. Howard and G. W. Johnson, *Solid-St. Electron.* **8**, 275 (1965).